Metamaterial-Inspired Electrically Small Antennas Integrated Into Structural Materials

Kelvin J. Nicholson
Aerospace Composite Technologies
DSTO - Fisherman's Bend
Melbourne, Australia
kelvin.nicholson@dsto.defence.gov.au

Thomas C. Baum and Kamran Ghorbani
Department of Electrical and Computer Engineering
RMIT University
Melbourne, Australia
thomas.baum@rmit.edu.au

Richard W. Ziolkowski
Department of Electrical and Computer Engineering
University of Arizona
Tucson, AZ, USA
ziolkowski@ece.arizona.edu

***Abstract*—An electrically small Egyptian axe dipole antenna has been designed and integrated into a glass fiber reinforced polymer (GFRP), a structural material now commonly found in most mobile platforms. The integration is accomplished by sewing the antenna with conductive threads into the GFRP prepreg and accounting for dimensional variations after curing under high temperature and pressure in an autoclave. The simulated and measured reflection coefficient values and radiated field patterns are in good agreement. These comparisons demonstrate that the antenna is nearly completely matched to the source without any matching circuit and radiates as an electric dipole.**

***Keywords*—electrically small antenna, metamaterial-inspired, glass fiber reinforced polymer**

I. Introduction

The recent interest in wireless healthcare monitoring for the aging population, sports and military applications has led to the design and realization of a variety of wearable antennas [1-6]. Advances have required understanding not only the conductive threads but also sewing techniques [7]. This interest has extended to flexible polymers [8, 9] that could be attached not only to the body or to textiles, but also to load-bearing structures. In this paper, we demonstrate an electrically small antenna fully integrated into a glass fiber reinforced polymer (GFRP) structure material. This choice enables the potential for antenna related systems to be fully integrated into mobile platforms such as automobiles, airplanes and ships, which are now commonly constructed from GFRP and carbon fiber reinforced polymer (CFRP) materials.

To achieve an electrically small antenna (ESA) design, the near-field resonant parasitic paradigm [10] was followed. In particular, we selected the Egyptian axe dipole (EAD) antenna. This ESA design was first introduced to achieve a Huygens source [11]. It has been subsequently used to achieve multi-frequency and circular polarized ESAs [12] and augmented with non-Foster circuits to achieve broad impedance bandwidth [13, 14]; large directivity bandwidth [15]; and an ESA that simultaneously is efficient, has large impedance and directivity bandwidths, and a large front-to-back-ratio [16]. As with other metamaterial-inspired NFRP ESAs [10], the EAD antenna engineered for integration into the GFRP material was optimized to be matched to a 50Ω source (by choice) with no matching circuit.

II. Antenna Design

All simulations were performed with the ANSYS/ANSOFT high frequency structure simulator, ANSYS HFSS. The EAD antenna designed for the GFRP integration is shown in an isometric view in Fig. 1(a). The NFRP EAD element is shown by itself in Fig. 1(b). Starting from a previous 300 MHz design [17], it was modified to accommodate the structural material properties. The EAD element was assumed to be 0.017 mm thick (0.5 oz) copper with the parameters ε_r = 1.0, μ_r = 0.999991 and $\sigma = 5.8\times 10^7$ S/m. Its outer radius was 76.0 mm; the width of its center trace was 10.0 mm; the width of its arc was 16.0 mm; and the length of its arms was 45.0 mm and their trace width was 10.0 mm. The gap between the arms was 29.0 mm. The GFRP material was modelled as HexPly914E [18] prepreg [19] with a thickness of 4.311 mm and measured electromagnetic parameters ε_r = 4.251, tan ϕ_{elec} = 0.0142, μ_r = 0.993, and tan ϕ_{mag} = 0.003. The driven dipole element is shown by itself in Fig. 1(c). In contrast to many previous EAD-based designs, which utilized lumped element inductors incorporated into the NFRP element for tuning purposes and a driven top-hat loaded dipole (i.e., another EAD element) for matching, the solid EAD element and the meanderline version of the driven dipole proved to be a simple yet effective approach to introduce the required inductance to achieve matching. This was necessitated in part because of the HexPly914E properties. The optimized total length was 86.0 mm. The length of each top edge of each half of the dipole in millimeters was 15, 6, 10, and 11.5. A lumped element port was placed across the remaining 1.0 mm gap. The design was tuned to achieve a target center frequency near to 300.0 MHz.

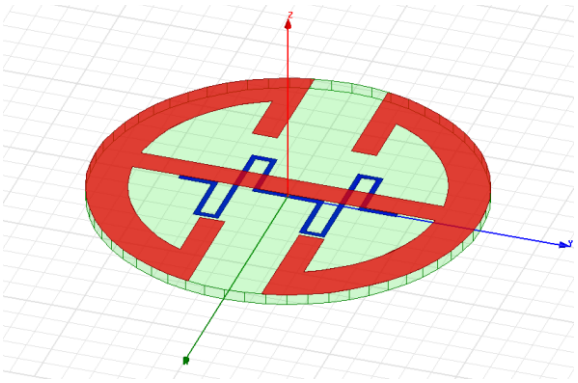

(a)

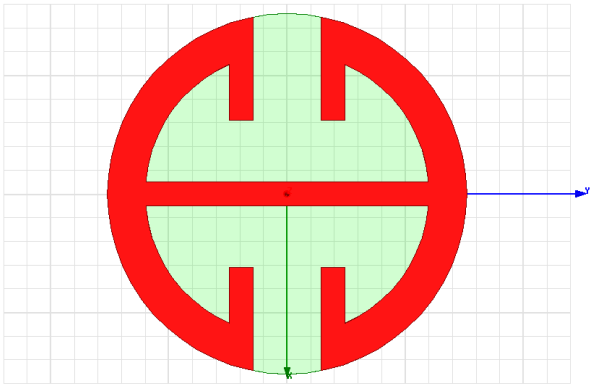

(b)

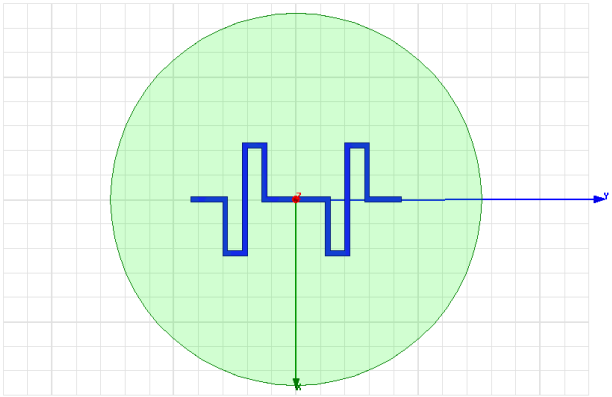

(c)

Fig. 1 The HFSS EAD NFRP antenna model. (a) Isometric view, (b) top NFRP layer view, and (c) bottom meanderline augmented driven dipole layer view.

The simulated properties of the antenna are shown in Fig. 2. The $|S_{11}|$ values for different source frequencies are shown in Fig. 2(a). The resonance frequency of the final design was f_{res} = 303.49 MHz with $|S_{11}|_{min}$ = –21.31 dB. Thus, if $k = 2\pi f_{res} / c$ is the free space wave number and a is the radius of the smallest sphere enclosing the antenna, then ka = 0.48, which confirms that the antenna is electrically small. The resistance and reactance values as functions of the source frequency are shown in Fig. 2(b). The shape of the reactance curve clearly shows the antenna is behaving as an electric antenna through the resonance frequency. The E- and H-plane directivity patterns at the resonance frequency are shown in Fig. 2(c). They clearly demonstrate that the antenna is acting as an electric dipole radiator. The calculated radiation efficiency at this frequency was 74%, as very reasonable value considering the large loss tangent of the HexPly914E disk layer.

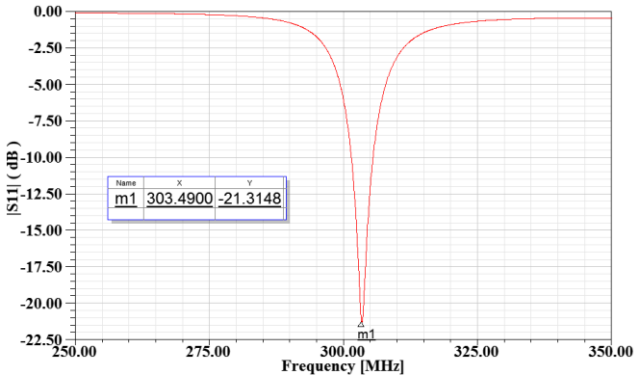

(a)

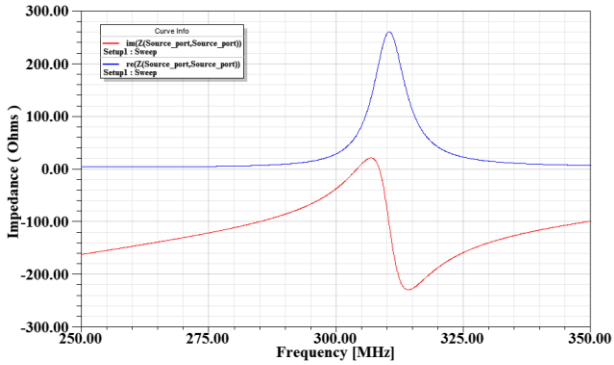

(b)

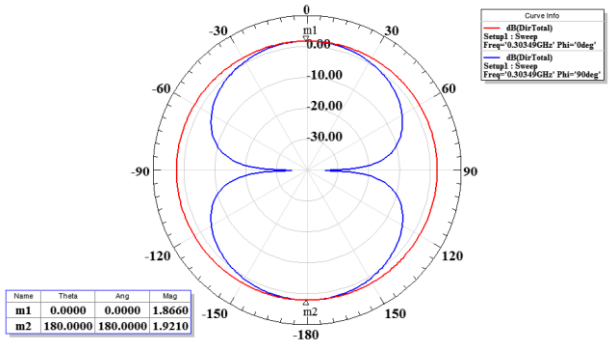

(c)

Fig. 2 HFSS simulation results. (a) $|S_{11}|$ values (dB) versus source frequency, (b) resistance (blue) and reactance (red) values versus the source frequency, and (c) the E-plane (blue) and H-plane (red) directivity patterns (dB) at the resonance frequency, 303.49 MHz. The maximum realized gain in the broadside direction was 0.50 dB.

III. MEASUREMENTS

The antenna was sewn directly into the prepreg (plain-weave S-2 glass fiber with an areal density of 48.0 $g.m^{-2}$ impregnated with the Hexply® 914E epoxy acquired from Hexcel, United States [18]) with a commercial digital sewing machine (Brother PR1000e [20]) using Shieldex 110/34f thread (a silver coated conductive filament) [21]. The prepreg was then cured under 700 kPa pressure for 1.0 hour using a $2°C.min^{-1}$ ramp rate.

(a)

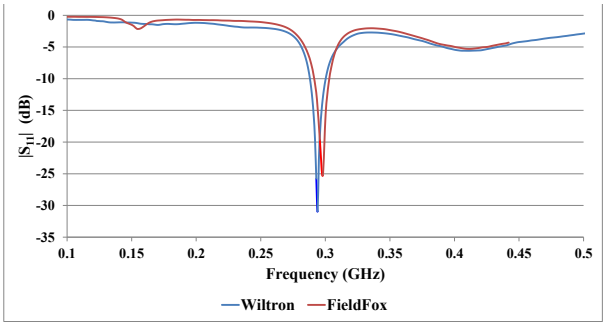

(b)

Fig. 3 Measurement of the substrate integrated EAD NFRP antenna. (a) View of the antenna in the RMIT anechoic chamber, and (b) $|S_{11}|$ values (dB) versus the source frequency.

The radiation characteristics of the antenna were measured in the RMIT anechoic chamber. The fabricated prototype antenna in the RMIT anechoic chamber is shown in Fig. 3(a). Using both the automatic Wiltron calibrated vector network analyzer (VNA) in the chamber and a calibrated Field Fox VNA [22] in the office, the measured $|S_{11}|$ values are shown in Fig. 3(b). Both sets of measured values are in very good agreement regardless of the measurement environment confirming that the antenna is resonant (given the low operating frequency and near-field proximity) near 300 MHz. Furthermore, the measured values are in good agreement with the numerical predictions. Despite pre-planning for it, the slight variation in the resonance frequency is associated with the warpage in the material that occurs during the autoclave curing process.

The measured maximum realized gain was approximately –5 dB, indicating a much larger loss than predicted. Through simulations and additional measurements, we have determined that this loss is associated with a much higher loss in the GFRP material and a much lower conductivity of the threads, both of which were much different from their advertised values. A second prototype based on improved materials is currently being measured. Those and related results for a sewn high impedance ground plane will be reviewed in our presentation.

ACKNOWLEDGMENTS

RWZ contributed to this work while he was the 2014-2015 Australian DSTO Fulbright Distinguished Chair in Advanced Science and Technology at DSTO-Fisherman's Bend. He would like to express a special thank you to DSTO and the Australian-American Fulbright Commission for their support.

REFERENCES

[1] L. Ma, R. M. Edwards, S. Bashir and M. I. Khattak, "A wearable flexible multi-band antenna based on a square slotted printed monopole," in *Proc. Loughborough Antennas Propag. Conf., LAPC 2008*, Loughborough, UK, Nov. 2008, pp. 345-348.

[2] L. Ma, R. M. Edwards and W. G. Whittow, "A notched hand wearable ultra wideband w printed monopole antenna for sporting activities," in *Proc. Loughborough Antennas Propag. Conf., LAPC 2008*, Loughborough, UK, Nov. 2008, pp. 397-400.

[3] N. H. M. Rais, P. J. Soh, F. Malek. S. Ahmad, N. Hashim and P. Hall, "A review of wearable antenna," in *Proc. 2009 Loughborough Antennas Propag. Conf., LAPC 2009*, Loughborough, UK, Nov. 2009, pp. 225-228.

[4] P. Hall, Y. Hao and S. Cotton, "Advances in antennas and propagation for body centric wireless communications," in *Proc. Fourth European Conf. Antennas Propag., EuCAP2010*, Barcelona, Spain, Apr. 2010, pp.1-7.

[5] L. Zhang, Z. Wang and J. L. Volakis, "Textile antennas and sensors for body-worn applications," *IEEE Antennas Wirel. Propag. Lett*., vol. 11, pp. 1690-1693, 2012.

[6] T. Kaufmann and C. Fumeaux, "Wearable textile half-mode substrate-integrated cavity antenna using embroided vias," *IEEE Antennas Wirel. Propag. Lett*., vol. 12, pp. 805-808, 2013.

[7] T. Kaufmann, I.-M. Fumeaux and C. Fumeaux, "Comparison of fabric and embroided dipole antennas," in *Proc. Seventh European Conf. Antennas Propag., EuCAP2013*, Gothenburg, Sweden, Apr. 2013, pp. 3252-3255.

[8] Z. Wang, L. Zhang, Y. Bayram and J. L. Volakis, "Embroidered E-fiber-polymer composites for conformal and load bearing antennas," in *Proc. IEEE Int. Symp. Antennas Propag., APSURSI2010*, Toronto, Canada, Jun. 2010, pp. 1-4.

[9] Z. Wang, L. Zhang, Y. Bayram and John L. Volakis, "Embroidered conductive fibers on polymer composite for conformal antennas," *IEEE Trans. Antennas Propag.*, vol. 60, no. 9, pp. 4141-4147, Sep. 2012.

[10] R. W. Ziolkowski, P. Jin and C.-C. Lin, "Metamaterial-inspired engineering of antennas," *Proc. IEEE*, vol. 99, no. 10, pp. 1720-1731, Oct. 2011.

[11] P. Jin and R. W. Ziolkowski, "Metamaterial-inspired, electrically small, Huygens sources," *IEEE Antennas Wirel. Propag. Lett.*, vol. 9, pp. 501-505, May 2010.

[12] P. Jin, C.-C. Lin and R. W. Ziolkowski, "Multi-functional, electrically small, planar near-field resonant parasitic antennas," *IEEE Antennas Wirel. Propag. Lett*., vol. 11, pp. 200-204, 2012.

[13] N. Zhu and R. W. Ziolkowski, "Broad bandwidth, electrically small antenna augmented with an internal non-Foster element," *IEEE Antennas Wireless Propag. Lett.*, vol. 11, pp. 1116-1120, 2012

[14] N. Zhu and R. W. Ziolkowski, "Broad bandwidth, electrically small, non-Foster element-augmented antenna designs, analyses, and measurements," *IEICE Trans. Commun.*, vol. E96-B, no.10, pp. 2399-2409, Oct. 2013.

[15] M.-C. Tang, N. Zhu and R. W. Ziolkowski, "Augmenting a modified Egyptian axe dipole antenna with non-Foster elements to enlarge its directivity bandwidth," *IEEE Antennas Wirel. Propag. Lett.*, vol. 12, pp. 421-424, 2013.

[16] R. W. Ziolkowski, M.-C. Tang and N. Zhu, "An efficient, broad bandwidth, high directivity, electrically small antenna," *Microw. Opt. Technol. Lett*., vol. 55, no. 6, pp. 1430-1434, June 2013.

[17] M.-C. Tang and R. W. Ziolkowski, "Improving the directivity of electrically small antennas using a slot-modified, finite, parasitic ground plane," *IEEE Access*, vol. 1, pp. 16-28, May 2013.

[18] http://www.hexcel.com/Resources/DataSheets/Prepreg-Data-Sheets/914_eu.pdf

[19] J. R. Hazen and D. K. Dawson, *Aerospace Composites: A Design & Manufacturing Guide*, 1st Ed, Garner Publications, Inc., Wheat Ridge, CO, 2007.

[20] http://welcome.brother.com/ae-en/products-services/home-sewing-machines/pr-1000.html

[21] http://www.shieldextrading.net/pdfs/11034x2%20HC.pdf

[22] http://www.keysight.com/en/pc-1742042/fieldfox-handheld-rf-and-microwave-analyzers?cc=US&lc=eng